Bandgap Engineering in CZTSSe Thin Films via Controlling S/(S+Se) Ratio

Vijay C. Karade[1),2)] · Jun Sung Jang[2)] · Kuldeep Singh Gour[3)] · Yeonwoo Park[1)] · Hyeonwook Park[4)] ·
Jin Hyeok Kim[2)]* · Jae Ho Yun[1)]*

[1)]Department of Energy Engineering, Korea Institute of Energy Technology (KENTECH), Naju, 522132, Korea
[2)]Optoelectronics Convergence Research Center and Department of Materials Science and Engineering, Chonnam National University, Gwangju, 61186, Korea
[3)]Surface Engineering Group, Advanced Materials & Processes Division, CSIR-National Metallurgical Laboratory, Jamshedpur, 831007, India
[4)]Department of Hydrogen Energy, Korea Institute of Energy Technology (KENTECH), Naju, 522132, Korea

ABSTRACT: The earth-abundant element-based $Cu_2ZnSn(S,Se)_4$ (CZTSSe) thin film solar cells (TFSCs) have attracted greater attention in the photovoltaic (PV) community due to their rapid development in device power conversion efficiency (PCE) >13%. In the present work, we demonstrated the fine-tuning of the bandgap in the CZTSSe TFSCs by altering the sulfur (S) to the selenium (Se) chalcogenide ratio. To achieve this, the CZTSSe absorber layers are fabricated with different S/(S+Se) ratios from 0.02 to 0.08 of their weight percentage. Further compositional, morphological, and optoelectronic properties are studied using various characterization techniques. It is observed that the change in the S/(S+Se) ratios has minimal impact on the overall Cu/(Zn+Sn) composition ratio. In contrast, the S and Se content within the CZTSSe absorber layer gets altered with a change in the S/(S+Se) ratio. It also influences the overall absorber quality and gets worse at higher S/(S+Se). Furthermore, the device performance evaluated for similar CZTSSe TFSCs showed a linear increase and decrease in the open circuit voltage (V_{oc}) and short circuit current density (J_{sc}) of the device with an increasing S/(S+Se) ratio. The external quantum efficiency (EQE) measured also exhibited a linear blue shift in absorption edge, increasing the bandgap from 1.056 eV to 1.228 eV, respectively.

Key words: CZTSSe, Thin film solar cells, Bandgap engineering, Kesterite, Doping

1. Introduction

The growing energy demands in forthcoming years to reach almost 30-40 terawatts are predicted by the year 2050[1, 2]. Therefore, finding sustainable energy sources that can overcome carbon emissions and fulfill energy demands is necessary. Solar energy can be a suitable renewable source of energy that can satisfy these demands. The CIGS and CdTe thin film solar cells (TFSCs) have already achieved device power conversion efficiency (PCE) of over 22% and are already commercialized[3, 4]. However, the toxicity of Cadmium (Cd) and scarcity of Indium (In) and Gallium (Ga) elements encouraged the researcher to develop an earth-abundant element-based, low-cost, and nontoxic element-based alternative absorber layer[5-7]. Accordingly, the kesterite-based $Cu_2ZnSn(S_x,Se_{1-x})$ CZTSSe absorber layer exhibits

earth-abundant elements, high absorption coefficient ($10^5 \, cm^{-1}$), a tunable bandgap (E_g) ranges from 1.0 to 1.5 eV, and making them one of the suitable light absorber materials for TFSCs[8, 9].

Recently, CZTSSe-based TFSCs have achieved a record PCE of 13.8%[10]. However, the device performance of pure sulfide-based Cu_2ZnSnS_4 (CZTS) having record PCE = ~11.0%, pure selenide-based $Cu_2ZnSnSe_4$ (CZTSe) having record PCE = ~12.5%, and mixed chalcogenide (CZTSSe) is limited by the formation of defects, secondary phases, and associated charge carrier recombinations[11, 12]. Most of the record efficiency devices exhibit non-stochiometric Cu-poor and Zn-rich conditions. At the same time various secondary phases, such as Cu_2SnS/Se_3 (CTS/Se), CuS/Se, ZnS/Se, and SnS/Se have also been observed in this Cu-poor and Zn-rich composition conditions[11, 13]. They mainly originate from thermodynamically unstable single phases of CZTS and sulfur (S) rich conditions[14, 15]. Although pure sulfide CZTS-based devices exhibit a wider E_g of 1.5 eV, they typically suffer a higher open-circuit voltage (V_{oc}) loss[8]. On the

*Corresponding author: jhyun@kentech.ac.kr (Jae Ho Yun);
jinhyeok@chonnam.ac.kr (Jin Hyeok Kim)

other hand, pure selenide CZTSe-based device has a narrow E_g of 1.0 eV than the theoretically estimated maximum PCE of kesterite device (~32%), limiting their further development[16]. Lately, kesterite CZTSSe-based TFSCs have demonstrated their applicability in tandem configuration[17, 18]. To employ kesterite absorbers in tandem solar cell device applications, it is essential to finely tune their E_g for efficient light absorption. Therefore, having a suitable E_g, optimum S/(S+Se) ratio, and fine E_g tuning strategies are needed for efficient light harvesting in PV devices.

In this work, the CZTSSe absorber layers were successfully deposited by the direct-current (DC) sputtering method, and a fine-tuning of the E_g was done by altering the S/(S+Se) ratio. Firstly, the composition and morphological properties of the CZTSSe absorber layer were evaluated, and later on, the influence of the S/(S+Se) ratio on optoelectronic properties was investigated by fabricating CZTSSe TFSCs with different S/(S+Se) ratio. The detailed investigation and obtained results are discussed below.

2. Materials and Methods

2.1 Stacked Metallic precursor preparation

The molybdenum (Mo) coated soda-lime glass (SLG) substrates of 2.5 × 2.5 cm^2 were cleaned with an ultrasonication process sequentially with isopropyl alcohol (IPA) and deionized (DI) water for 15 min and dried under a nitrogen gun. Further, the cleaned Mo substrates were subjected to DC sputtering, and a precursor with stacking order of Cu/Sn/Zn/Mo was prepared. The sputtering power of 0.68 W/cm^2 was used for all the targets while sputtering. Pure metallic targets with 99.999% purity purchased from (i-TASCO, USA) were used for all the processes.

2.2 CZTSSe absorber preparation

The prepared precursor layers were initially soft-annealed at 300°C for 60 min in an Ar atmosphere within the tube furnace. Soft-annealed precursor thin films were annealed in a chalcogenide atmosphere with mixed S and Se powder (0.2 gm). The chamber was first evacuated to a base pressure of 1.0×10^{-5} Torr and then controlled up to 500 Torr using Ar gas before the annealing process. After that, the chamber was heated up to 520°C with a ramping rate of 10°C/s, and the temperature was maintained for 8 min. The S/(S+Se) ratio of powder was changed from 0.02 to 0.08 to prepare the CZTSSe absorber thin films with different E_g. This 0.02 gm of S powder was mixed in 1.00 gm of Se chunks and grind well to make it homogeneous. Similarly, other powders

were prepared by changing the S amount. It should be noted that all the samples were sulfo-selenized at the same conditions with the same amount of powder.

2.3 Device fabrication process

The CZTSSe devices were successfully fabricated by depositing the multi-layered structure of Al/AZO/*i*-ZnO/CdS/CZTSSe/Mo/ SLG. The p-n junction was fabricated by depositing a ~60 nm thick CdS as a buffer layer using the chemical bath deposition (CBD) technique. The deposition was performed with a precursor of 1.5 mM CdSO$_4$, 2.871 M ammonia, and 50 mM thiourea at 60°C for 14 min and then rinsed in DI water. Further, the transparent conducting oxide (TCO) layers, i.e., *i*-ZnO and Al-doped ZnO-based (AZO), were deposited by radio-frequency (RF) sputtering technique at room temperature (RT) and 350°C (real temperature 210-220°C), respectively. The thickness of *i*-ZnO and AZO were maintained at 30 and 550 nm, respectively. Finally, the Al top grid (1 μm) was deposited using the DC sputtering technique with the active area of the fabricated CZTSSe TFSCs to 0.30 cm^2. Detailed thin film deposition and device fabrication processes can be found in our previous reports[19, 20].

2.4 Analysis of CZTSSe thin films and devices

The compositional ratio of the CZTSSe thin films was characterized by an X-ray fluorescence (XRF) spectroscopy (Axios Minerals PANalytical Netherlands). The surface morphology of the thin films was characterized using a field emission scanning electron microscope (FE-SEM, Model: JEOL JSM-6701F, Japan). The PCE for solar cell devices was characterized by a class AAA solar simulator (WXS-155S-L2) with the condition of AM 1.5G, 100 mW/cm^2, and 25°C. The devices' external quantum efficiency (EQE) was measured using a QEX10 spectral response system (S-9230, SOMA Optics, Japan).

3. Results and discussion

3.1 Compositional and morphological properties

To determine the effect of the S/Se ratio on the composition ratio of the CZTSSe absorber layers XRF measurements were performed, and the corresponding results are shown in Fig. 1 (a)-(d). It shows that, with the change in the S/Se ratio during the sulfo-selenization process, the relative metal composition ratio Cu/(Zn+Sn) remained nearly stable ~0.65 - 0.66. At the same time, the Cu/Sn and Zn/Sn ratios increased initially with

increasing the S/Se ratio from 0.02 to 0.06 and then decreased to a higher S/Se ratio of 0.08 (Fig. 2 (a)). The Zn/Sn ratio increased from 1.35 to 1.39 and then reduced to 1.36. Similarly, the Cu/Sn ratio increased from 1.40 to 1.44 and decreased slightly to 1.43 (Fig. 1 (b)). In the case of the chalcogenide to metal (S+Se/M) composition ratio, it nearly remained constant (Fig. 1 (c))[14]. The S/(S+Se) and Se/(S+Se) ratios also increased and decreased linearly with an increase in S and a decrease in Se content within the CZTSSe absorber layer, respectively (Fig. 1 (d))[15]. During the experiment, the metal (Cu-Zn-Sn) composition ratios for all the precursor layers were kept constant; thus, the change in the S/Se ratio was not significantly influenced. However, the possible formation of various secondary phases such as ZnS/Se, $Cu_2Sn(S/Se)_3$, and Cu(S/Se), potentially affected the Zn/Sn and Cu/Sn ratios[11]. The occurrence of these secondary phases is attributed to the thermodynamically unstable nature of CZTSe and CZTS absorbers due to their off-stoichiometry composition and a higher S/(S+Se) ratio[21, 22]. Further, for the sulfo-selenization process, a fixed amount of S/Se mixture powder (0.2 gm) was used; hence the relative (S+Se)/M composition ratio for the

CZTSSe absorber layer also remained constant. These measurements shows that can be seen that the overall composition ratios of the absorber layer do not get deflated by the change in the relative S/(S+Se) ratio[23].

Fig. 2 (a)-(d) shows surface FE-SEM images of the CZTSSe thin films fabricated with different S/Se ratios. Surprisingly even though the metal composition of the precursor layers didn't change after the sulfo-selenization process, the changes in the absorber morphology with the different S/Se ratios were observed. At a lower ratio of 0.02, the CZTSSe absorber shows much larger grains with compact morphology. While, at a higher S/Se ratio of 0.08, the density of smaller grains and voids increased. This poor morphology, associated with increased S/Se ratio, may be attributed to higher S content in CZTSSe thin films and a shorter sulfo-selenization time during the rapid thermal annealing (RTA) process[15]. These smaller grains increase defects and grain boundary density in the kesterite CZTSSe absorbers and can contribute to higher carrier recombination reducing device performance[12, 25, 26].
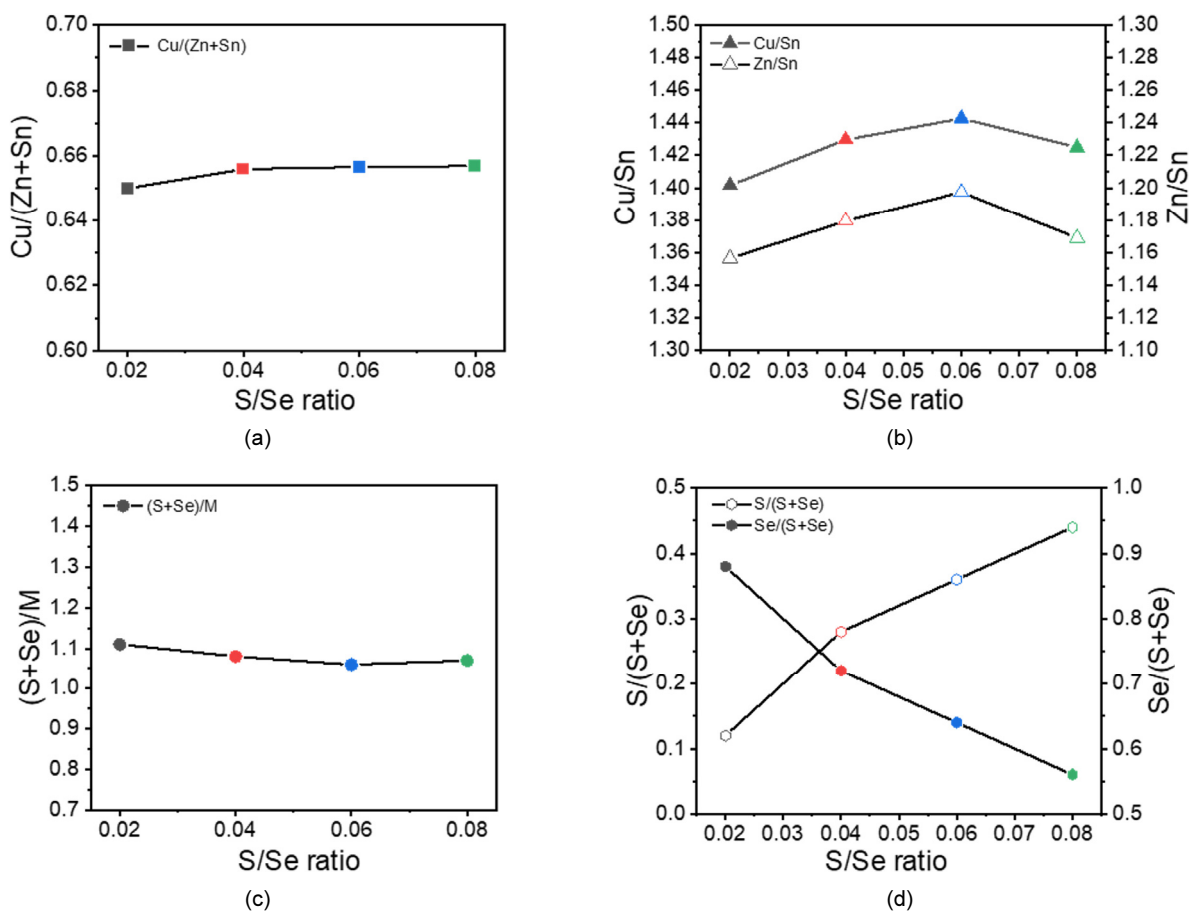

Fig. 1. The chemical composition ratios of the CZTSSe thin films (a) Cu/(Zn+Sn), (b) Cu/Sn and Zn/Sn, (c) (S+Se)/M, and (d) S/(S+Se) and Se/(S+Se) measured by XRF.
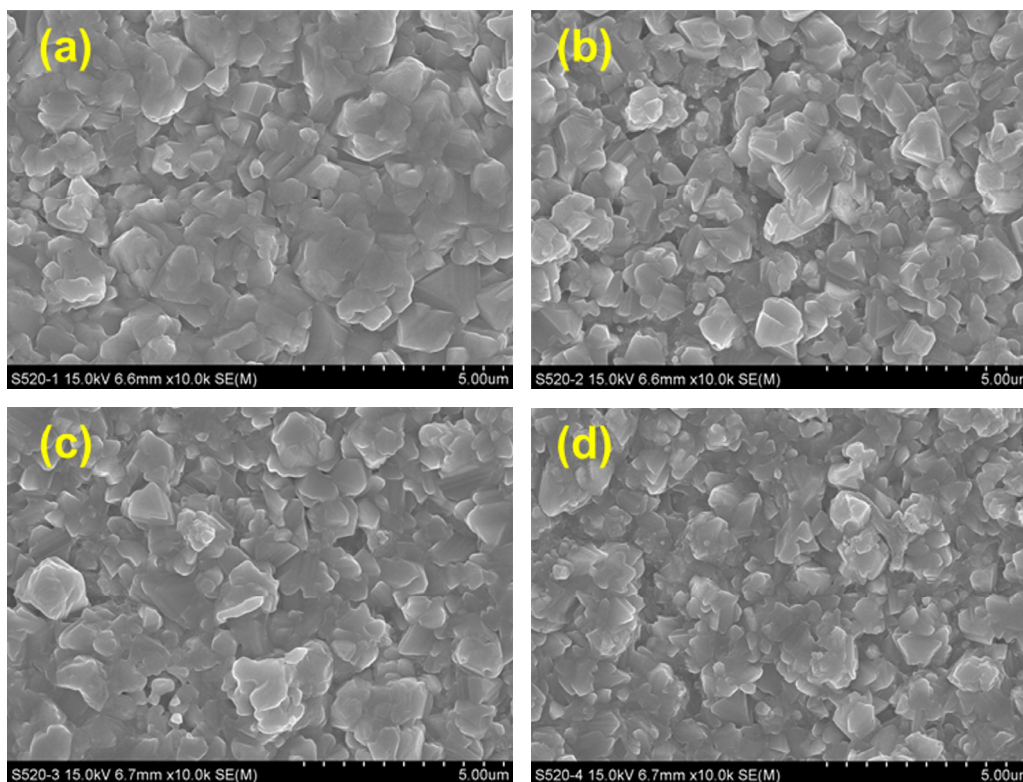
Fig. 2. Surface FESEM images of the CZTSSe absorber thin films prepared with (a) 0.02, (b) 0.04, (c) 0.06, and (d) 0.08 S/Se ratio

3.2 Optical and electrical properties

To further evaluate the effect of the S/Se ratio on the performance of the CZTSSe devices, the device performance was measured under STC, and the corresponding data is shown in Fig. 3. As can be seen in the figure, the V_{oc} and short circuit current density (J_{sc}) of the CZTSSe devices get linearly increased and decreased with increasing the S/Se ratio from 0.02 to 0.08, respectively. At the lower S/Se ratio of 0.02, the average V_{oc} of the device remained up to 439 mV which increased further to 460 and 489 mV for 0.04 and 0.06 S/Se ratios, respectively (Fig. 3 (a)). When the ratio increased to 0.08, the V_{oc} of the CZTSSe devices reached over 500 mV delivering an average V_{oc} of 506 mV. It is known that the V_{oc} is directly related to the E_g of absorber materials; therefore, increasing S content leads to an increase in E_g and an increase in V_{oc} of the CZTSSe device[14, 27]. On the other hand, the average J_{sc} of the devices decreased linearly from 34.3 to 29.04 mA/cm^2 when the S/Se ratio increased from 0.02 to 0.06 (Fig. 3 (b)). The highest ratio of 0.08 marginally reduced up to 27.99 mA/cm^2. The change in E_g values is the reason for the increase in V_{oc} and decreases in J_{sc} values for different S/Se ratios[27]. The average fill factor (FF) of the CZTSSe devices initially reduced from 54% to 44%, whereas it increased marginally to 50% (Fig. 3 (c)). Following

the same trend, the average PCE of CZTSSe devices also decreased from 8.17% to 6.26%, from 0.02 to 0.06, respectively, and increased slightly to 7.01% at a S/Se ratio of 0.08 (Fig. 3 (d)). The series resistance (R_s) in the device also increased nearly two times from 11.2 Ω to 22.05 Ω with an increase in the S/Se ratio, while it decreased slightly to 17.5 Ω at 0.08. The shunt resistance (R_{sh}) also increased and decreased with increasing ratio. The increased R_s can be observed due to the formation of resistive Mo(S,Se)$_2$ layer, degradation of absorber quality and possible formation of shunt paths near junction reason. The exact reason for this abnormal behavior is not known, though some additional investigations are needed. There is a tradeoff between the R_s and R_{sh} in devices. This initial decrease in FF and PCE could be attributed to the poor p-n heterojunction quality of the CZTSSe devices. The changes in the E_g values also vary the conduction band offset (CBO) values, and the possible increase in the CBO could severely impact the FF and PCE of CZTSSe devices[28, 29]. The sudden increased device performance after degradation of FF and PCE can also be explained by the relatively lower R_s and higher R_{sh} values at 0.08 ratio, thus marginally high PCE and FF was observed. In kesterites, Zn-rich and Cu-poor case, highly resistive Zn-related secondary phases (ZnS/Se) are commonly observed which possess a wide
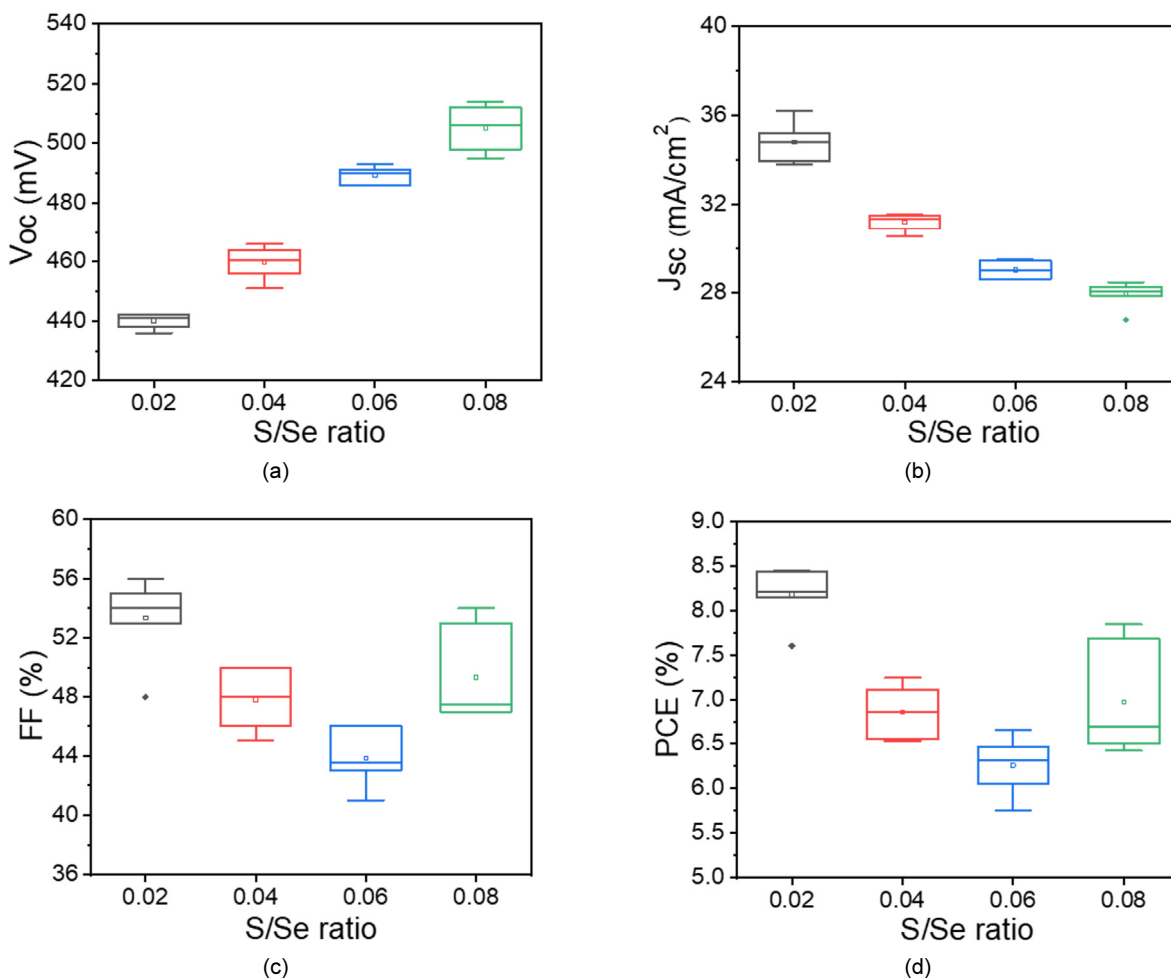
Fig. 3. (a) V_{oc}, (b) J_{sc}, (c) FF, and (d) PCE of the CZTSSe devices prepared with 0.02-0.08 S/Se ratio

E_g, consequently, they lead to a degradation in the PCE of CZTSSe TFSCs[22, 24]. The highest device PCE of 8.46% was achieved with a S/Se ratio of 0.02% with V_{oc}, J_{sc}, and FF of 442 mV, 33.99 mA/cm^2, and 56%, respectively. Where the highest V_{oc} of 514 mV was achieved with the highest S/Se ratio of 0.08, the corresponding device exhibits the highest PCE of 7.85%.

Fig. 4 (a) and Table 1 show the corresponding current-density-voltage (J-V) curves and device parameters. To validate the changes in E_g values with different S/Se ratios, the external quantum efficiency (EQE) for best-performing devices was measured. As shown in Fig. 4 (b), all the devices show strong absorption in the ultraviolet-visible (UV-Vis) region, ranging from 350 to 780 nm, decreasing further in the longer wavelength. All the samples exhibit a maximum EQE response greater than 80% without antireflection coating (ARC). With the increase in the S/Se ratio from 0.02 to 0.08, a significant shift in the absorption edge by approximately 200 nm in the longer region from ~1000 to 1190 nm was observed[14]. This blue shift

corroborates well with the change in E_g values estimated by tracing the inflection point of the EQE spectrum at the absorption edge (Fig. 4 (c)). The E_g values increased linearly from 1.056 to 1.228 eV linearly with increasing S/Se ratio from 0.02 to 0.08, respectively (Fig. 4 (d)). It has been shown that, as the S content in the CZTSSe thin films increases, it shifts the valence band maximum position towards higher binding energy side resulting in widening of E_g.

In one study, *Singh et al.*[23] fabricated the CZTSSe thin films and investigated how the small amount of S and Se can control the E_g. They observed that with the increase in selenization time, the E_g decreases from 1.35 to 1.10 eV, due to the replacement of S by Se, respectively. Similarly, *Kim et al.*[14] studied the effect of S/(S+Se) ratios on E_g and their influence on the formation of secondary phases of the CZTSSe solar cells. They also observed formation (960 nm) of thick $Mo(S,Se)_2$ resulted in decrease in the S/(S+Se) ratio that led to poor carrier collection at the back interface.
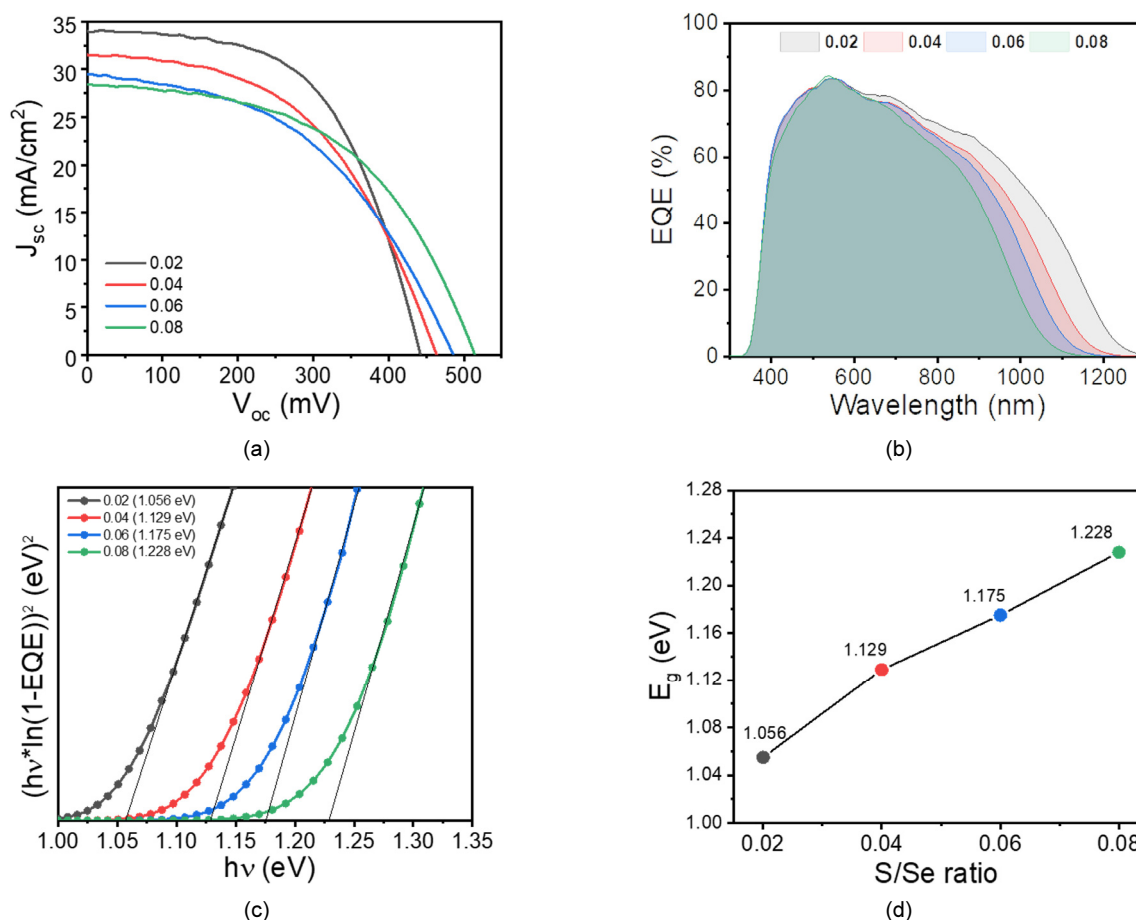
Fig. 4. (a) Light J-V curve, (b) external quantum efficiency (EQE), (c) estimated bandgap (E_g) from EQE, and (d) linear plot of estimated E_g and S/Se ratio from the CZTSSe devices prepared with 0.02-0.08 S/Se ratio

Table 1. Device parameters of the CZTSSe devices prepared with 0.02-0.08 S/Se ratio

Sample code		V_{oc} (mV)	J_{sc} (mA/cm^2)	FF (%)	PCE (%)	R_S (Ω)	R_{Sh} (Ω)	E_g (EQE) eV
0.02	Avg.	439 ± 3	34.31 ± 0.5	54 ± 2	8.17 ± 0.5	11.20 ± 2	499 ± 400	1.056
	Best	442	33.99	56	8.46	10.27	116	
0.04	Avg.	460 ± 4	31.22 ± 0.6	48 ± 2	6.87 ± 0.4	16.70 ± 1.4	1121 ± 600	1.129
	Best	464	31.52	50	7.25	15.61	500	
0.06	Avg.	489 ± 4	29.04 ± 0.7	44 ± 2	6.26 ± 0.4	22.05 ± 3.8	487 ± 300	1.175
	Best	486	29.48	46	6.65	19.72	833	
0.08	Avg.	506 ± 8	27.99 ± 1.5	50 ± 4	7.01 ± 0.7	17.32 ± 4	509 ± 100	1.228
	Best	514	28.49	54	7.85	13.92	500	

4. Conclusions

In the present work, we have successfully demonstrated that the E_g of the CZTSSe devices can be finely tuned by changing the S/(S+Se) ratio. It was found that the change in the S/Se ratio from 0.02 to 0.08 does not modify the overall Cu/(Zn+Sn) metal composition ratio. While, S/(S+Se) and Se/(S+Se) within the CZTSSe absorber layer get linearly increased and decreased,

respectively. The morphological studies revealed, the density of smaller grains also increased, and overall absorber quality decreased at a higher S/(S+Se) ratio for CZTSSe absorbers. The optical and electronic properties estimated for corresponding devices showed that the V_{oc} and J_{sc} of the CZTSSe device also increased and decreased linearly with increasing the S/(S+Se) ratio. Further E_g values estimated from EQE showed a linear increase from 1.056 eV to 1.228 eV. The device PCE also gets

degraded with increase in S/(S+Se) ratio, thus fine tuning of composition with an increase in the E_g, suitable CdS buffer layer thickness, and optimization of CBO are needed. It can produce high quality CZTSSe device with an improved carrier separation process. This study will help E_g engineering the CZTSSe absorber, making it highly suitable for next-generation tandem solar cell applications.

Conflict of Interest

The authors have no conflict of interest to declare.

Acknowledgment

References

1. Song, S., Lin, H., Sherman, P., Yang, X., Chen, S., Lu, X., Lu, T., Chen, X., McElroy, M. B., "Deep Decarbonization of the Indian Economy: 2050 Prospects for Wind, Solar, and Green Hydrogen," iScience 2022, 25(6), 104399. https://doi.org/10.1016/j.isci.2022.104399.

2. van Ruijven, B. J., De Cian, E., Sue Wing, I., "Amplification of Future Energy Demand Growth Due to Climate Change," Nat. Commun, 10(1), 2762 (2019). https://doi.org/10.1038/s41467-019-10399-3.

3. Nakamura, M., Yamaguchi, K., Kimoto, Y., Yasaki, Y., Kato, T., Sugimoto, H., "Cd-Free Cu(In,Ga)(Se,S) 2 Thin-Film Solar Cell With Record Efficiency of 23.35%," IEEE J. Photovoltaics, 9(6), 1863-1867 (2019). https://doi.org/10.1109/JPHOTOV.2019.2937218.

4. Shin, D., Saparov, B., Mitzi, D. B., "Defect Engineering in Multinary Earth-Abundant Chalcogenide Photovoltaic Materials," Adv. Energy Mater., 7(11), 1602366 (2017). https://doi.org/10.1002/aenm.201602366.

5. Karade, V. C., Sutar, S. S., Shin, S. W., Suryawanshi, M. P., Jang, J. S., Gour, K. S., Kamat, R. K., Yun, J. H., Dongale, T. D., Kim, J. H., "Machine Learning Assisted Analysis, Prediction, and Fabrication of High-Efficiency CZTSSe Thin Film Solar Cells," Adv. Funct. Mater. (2023). https://doi.org/10.1002/adfm.202303459.

6. Gong, Y., Zhu, Q., Li, B., Wang, S., Duan, B., Lou, L., Xiang, C., Jedlicka, E., Giridharagopal, R., Zhou, Y., Dai, Q., Yan, W., Chen, S., Meng, Q., Xin, H., "Elemental De-Mixing-Induced Epitaxial Kesterite/CdS Interface Enabling 13%-Efficiency Kesterite Solar Cells," Nat. Energy, 7(10), 966-977 (2022). https://doi.org/10.1038/s41560-022-01132-4.

7. Karade, V. C., Lim, J., Gour, K. S., Jang, J. S., Shin, S. J., Kim, J. H., Yang, B. S., Choi, H., Enkhbat, T., Kim, J., Yun, J. S., Jang, H. N., Yun, J. H., Park, J., Kim, J. H., "Overcoming the Limitations of Low-Bandgap Cu 2 ZnSn(S,Se) 4 Devices under Indoor Light Conditions: From Design to Prototype IoT Application," J. Mater. Chem. A, 10(44), 23831-23842 (2022). https://doi.org/10.1039/D2TA06565G.

8. Gour, K. S., Karade, V., Babar, P., Park, J., Lee, D. M., Singh, V. N., Kim, J. H., "Potential Role of Kesterites in Development of Earth-Abundant Elements-Based Next Generation Technology," Sol. RRL, 5(4), 2000815 (2021). https://doi.org/10.1002/solr.202000815.

9. Park, J., Yoo, H., Karade, V., Gour, K. S., Choi, E., Kim, M., Hao, X., Shin, S. J., Kim, J., Shim, H., Kim, D., Kim, J. hyeok, Yun, J., Kim, J. hyeok., "Investigation of Low Intensity Light Performances of Kesterite CZTSe, CZTSSe, and CZTS Thin Film Solar Cells for Indoor Applications," J. Mater. Chem. A, 8 (29), 14538-14544 (2020). https://doi.org/10.1039/D0TA04863A.

10. Zhou, J., Xu, X., Wu, H., Wang, J., Lou, L., Yin, K., Gong, Y., Shi, J., Luo, Y., Li, D., Xin, H., Meng, Q., "Control of the Phase Evolution of Kesterite by Tuning of the Selenium Partial Pressure for Solar Cells with 13.8% Certified Efficiency," Nat. Energy, 8(5), 526-535 (2023). https://doi.org/10.1038/s41560-023-01251-6.

11. Kumar, M., Dubey, A., Adhikari, N., Venkatesan, S., Qiao, Q., "Strategic Review of Secondary Phases, Defects and Defect-Complexes in Kesterite CZTS-Se Solar Cells. Energy Environ," Sci., 8(11), 3134-3159 (2015). https://doi.org/10.1039/C5EE02153G.

12. Kaur, K., Kumar, N., Kumar, M., "Strategic Review of Interface Carrier Recombination in Earth Abundant Cu-Zn-Sn-S-Se Solar Cells: Current Challenges and Future Prospects," J. Mater. Chem. A, 5(7), 3069-3090 (2017). https://doi.org/10.1039/C6TA10543B.

13. Chen, S., Gong, X. G., Walsh, A., Wei, S.-H., "Defect Physics of the Kesterite Thin-Film Solar Cell Absorber Cu2ZnSnS4," Appl. Phys. Lett., 96(2), 021902 (2010). https://doi.org/10.1063/1.3275796.

14. Kim, Y.-C., Jeong, H.-J., Lee, S. K., Kim, S.-T., Jang, J.-H., "The Effect of S/(S+Se) Ratios on the Formation of Secondary Phases in the Band Gap Graded Cu2ZnSn(S,Se)4 Thin Film Solar Cells," J. Alloys Compd., 793, 289-294 (2019). https://doi.org/10.1016/j.jallcom.2019.04.118.

15. Yu, J., Deng, H., Zhang, Q., Tao, J., Sun, L., Yang, P., Chu, J., "The Role of Tuning Se/(S + Se) Ratio in the Improvement of Cu2MnSn(S, Se)4 Thin Films Properties and Photovoltaic Device Performance," Sol. Energy, 179, 279-285 (2019). https://doi.org/10.1016/j.solener.2018.12.076.

16. Shockley, W., "Queisser, H. J. Detailed Balance Limit of

Efficiency of P-n Junction Solar Cells," J. Appl. Phys., 32(3), 510-519 (1961). https://doi.org/10.1063/1.1736034.

17. Gohri, S., Madan, J., Pandey, R., Sharma, R., "Design and Analysis of Lead-Free Perovskite-CZTSSe Based Tandem Solar Cell," Opt. Quantum Electron., 55(2), 171 (2023). https://doi.org/10.1007/s11082-022-04381-5.

18. Wang, D., Guo, H., Wu, X., Deng, X., Li, F., Li, Z., Lin, F., Zhu, Z., Zhang, Y., Xu, B., Jen, A. K. -Y., "Interfacial Engineering of Wide-Bandgap Perovskites for Efficient Perovskite/CZTSSe Tandem Solar Cells," Adv. Funct. Mater., 32(2), 2107359 (2022). https://doi.org/10.1002/adfm.202107359.

19. Karade, V. C., Suryawanshi, M. P., Jang, J. S., Gour, K. S., Jang, S., Park, J., Kim, J. H., Shin, S. W., "Understanding Defects and Band Tailing Characteristics and Their Impact on the Device Performance of Cu 2 ZnSn(S,Se) 4 Solar Cells," J. Mater. Chem. A, 10 (15), 8466-8478 (2022). https://doi.org/10.1039/D2TA00165A.

20. Karade, V., Choi, E., Gang, M. G., Yoo, H., Lokhande, A., Babar, P., Jang, J. S., Seidel, J., Yun, J. S., Park, J., Kim, J. H., "Achieving Low V OC -Deficit Characteristics in Cu 2 ZnSn (S,Se) 4 Solar Cells through Improved Carrier Separation," ACS Appl. Mater. Interfaces, 13(1), 429-437 (2021). https://doi.org/10.1021/acsami.0c16936.

21. Xie, H., Dimitrievska, M., Fontané, X., Sánchez, Y., López-Marino, S., Izquierdo-Roca, V., Bermúdez, V., Pérez-Rodríguez, A., Saucedo, E., "Formation and Impact of Secondary Phases in Cu-Poor Zn-Rich Cu2ZnSn(S1−Se)4 (0≤y≤1) Based Solar Cells," Sol. Energy Mater. Sol. Cells, 140, 289-298 (2015). https://doi.org/10.1016/j.solmat.2015.04.023.

22. Li, J., Kim, S. Y., Nam, D., Liu, X., Kim, J. H., Cheong, H., Liu, W., Li, H., Sun, Y., Zhang, Y., "Tailoring the Defects and Carrier Density for beyond 10% Efficient CZTSe Thin Film Solar Cells," Sol. Energy Mater. Sol. Cells, 159, 447-455 (2017). https://doi.org/10.1016/J.SOLMAT.2016.09.034.

23. Singh, O. P., Vijayan, N., Sood, K. N., Singh, B. P., Singh, V. N., "Controlled Substitution of S by Se in Reactively Sputtered CZTSSe Thin Films for Solar Cells," J. Alloys Compd., 648, 595-600 (2015). https://doi.org/10.1016/j.jallcom.2015.06.276.

24. Just, J., Sutter-Fella, C. M., Lützenkirchen-Hecht, D., Frahm, R., Schorr, S., Unold, T., "Secondary Phases and Their Influence on the Composition of the Kesterite Phase in CZTS and CZTSe Thin Films," Phys. Chem. Chem. Phys., 18(23), 15988-15994 (2016). https://doi.org/10.1039/C6CP00178E.

25. Sravani, L., Routray, S., Pradhan, K. P., Piedrahita, M. C., "Kesterite Thin-Film Solar Cell: Role of Grain Boundaries and Defects in Copper-Zinc-Tin-Sulfide and Copper-Zinc-Tin-Selenide," Phys. status solidi, 218(16), 2100039 (2021). https://doi.org/10.1002/pssa.202100039.

26. Nisika, Kaur, K., Kumar, M., "Progress and Prospects of CZTSSe/CdS Interface Engineering to Combat High Open-Circuit Voltage Deficit of Kesterite Photovoltaics: A Critical Review," J. Mater. Chem. A, 8(41), 21547-21584 (2020). https://doi.org/10.1039/d0ta06450e.

27. Zeng, C., Liang, Y., Zeng, L., Zhang, L., Zhou, J., Huang, P., Hong, R., "Effect of S/(S+Se) Ratio during the Annealing Process on the Performance of Cu2ZnSn(S,Se)4 Solar Cells Prepared by Sputtering from a Quaternary Target," Sol. Energy Mater. Sol. Cells, 203, 110167 (2019). https://doi.org/10.1016/j.solmat.2019.110167.

28. Lee, J., Enkhbat, T., Han, G., Sharif, M. H., Enkhbayar, E., Yoo, H., Kim, J. H., Kim, S. Y., Kim, J. H., "Over 11 % Efficient Eco-Friendly Kesterite Solar Cell: Effects of S-Enriched Surface of Cu2ZnSn(S,Se)4 Absorber and Band Gap Controlled (Zn,Sn)O Buffer," Nano Energy, 78, 105206 (2020). https://doi.org/10.1016/J.NANOEN.2020.105206.

29. Guo, H., Meng, R., Wang, G., Wang, S., Wu, L., Li, J., Wang, Z., Dong, J., Hao, X., Zhang, Y., "Band-Gap-Graded Cu 2 ZnSn(S,Se) 4 Drives Highly Efficient Solar Cells," Energy Environ. Sci., 15(2), 693-704 (2022). https://doi.org/10.1039/D1EE03134A.